

Journal Pre-proofs

Improving trade-offs in the figures of merit of gas-phase single-pass continuous CO₂ electrocatalytic reduction to formate

Guillermo Díaz-Sainz, Manuel Alvarez-Guerra, Beatriz Ávila-Bolívar, José Solla-Gullón, Vicente Montiel, Angel Irabien

PII: S1385-8947(20)33093-X
DOI: <https://doi.org/10.1016/j.cej.2020.126965>
Reference: CEJ 126965

To appear in: *Chemical Engineering Journal*

Received Date: 24 June 2020
Revised Date: 25 August 2020
Accepted Date: 6 September 2020

Please cite this article as: G. Díaz-Sainz, M. Alvarez-Guerra, B. Ávila-Bolívar, J. Solla-Gullón, V. Montiel, A. Irabien, Improving trade-offs in the figures of merit of gas-phase single-pass continuous CO₂ electrocatalytic reduction to formate, *Chemical Engineering Journal* (2020), doi: <https://doi.org/10.1016/j.cej.2020.126965>

This is a PDF file of an article that has undergone enhancements after acceptance, such as the addition of a cover page and metadata, and formatting for readability, but it is not yet the definitive version of record. This version will undergo additional copyediting, typesetting and review before it is published in its final form, but we are providing this version to give early visibility of the article. Please note that, during the production process, errors may be discovered which could affect the content, and all legal disclaimers that apply to the journal pertain.

© 2020 Published by Elsevier B.V.

© 2020. This manuscript version is made available under the CC-BY-NC-ND 4.0 license <http://creativecommons.org/licenses/by-nc-nd/4.0/>



Improving trade-offs in the figures of merit of gas-phase single-pass continuous CO₂ electrocatalytic reduction to formate

Guillermo Díaz-Sainz^{1*}, Manuel Alvarez-Guerra¹, Beatriz Ávila-Bolívar², José Solla-Gullón², Vicente Montiel², Angel Irabien¹

¹Chemical and Biomolecular Engineering Department, University of Cantabria, ETSIIT, Avda. Los Castros s/n, 39005, Santander, Spain

²Institute of Electrochemistry, University of Alicante, Apdo. 99, E-03080 Alicante, Spain

*Corresponding author: diazsg@unican.es

Abstract

The electrochemical conversion of CO₂ is gaining increasing attention because it could be considered as an appealing strategy for making value-added products at mild conditions from CO₂ captured. In this work, we report a process for the electrocatalytic reduction of CO₂ to formate (HCOO⁻) operating in a continuous way, employing a single pass of the reactants through the electrochemical reactor and using Bi carbon supported nanoparticles in the form of a membrane electrode assembly composed by a Gas Diffusion Electrode, a current collector and a cationic exchange membrane. This contribution presents the best trade-off between HCOO⁻ concentration, Faradaic Efficiency and energy consumption in the literature. We also show noteworthy values of energy consumption required of only 180 kWh·kmol⁻¹ of HCOO⁻, lower than previous approaches, working at current densities that allow achieving formate concentration higher than 300 g·L⁻¹ and simultaneously, a Faradaic Efficiency close to 90%. The results here displayed make the electrochemical approach closer for future implementation at the industrial scale.

Keywords

CO₂ electroreduction; Formate; Bismuth electrocatalysts; Gas Diffusion Electrode (GDE); Membrane electrode assembly (MEA); Electrochemical filter press reactor.

1. Introduction

The mitigation of CO₂ emissions to the atmosphere has promoted significantly the research interest in the field of electrocatalytic reduction of CO₂ towards chemicals with value added [1–9]. Among these CO₂ electroreduction reaction products, the formation of formic acid (HCOOH) or formate (HCOO⁻) (depending on pH value) is considered one of the most attractive carbon-based products [10], due to its interesting potential uses and its high world demand [11,12]. In particular, HCOOH production is estimated to be up to 0.950 Mt per year [13]. Apart from the traditional uses in several industries, HCOOH and HCOO⁻ are attracting attention as fuels in direct formic acid [14] or formate [15] fuel cells as well as one of the most promising materials for hydrogen storage [16].

This interest is reflected in the large number of studies in the field of CO₂ electrochemical reduction towards HCOOH or HCOO⁻ using different electrochemical configurations, operating conditions and catalyst material [17,18,27–30,19–26]. However, few studies have carried out the electrochemical reduction of CO₂ into HCOOH/HCOO⁻ in a continuous mode [31–40], which must be desirable from an industrial point of view [41,42]. Moreover, other requirements have to be considered for a practical implementation: high current densities supplied to the electrochemical filter press reactor [43], low overpotential for the electrocatalytic reduction of CO₂ towards HCOO⁻ to improve the energy efficiency [44,45] (electrochemical energy consumption less than 500 kWh per kmol of HCOO⁻), [42] high Faradaic Efficiency (FE) to obtain HCOO⁻ with high product selectivity and to avoid separation costs (more than 50%) [46]; and the electrochemical reactor should be scaled up to match other industrial processes [11]. High HCOOH/HCOO⁻ concentrations, as close as possible to 85% wt, the most common concentration in the market [47], are also necessary not just to assure economic viability of the process, but also because recent analyses of the environmental sustainability of

HCOO⁻ production by electroreduction of CO₂ alert that the energy requirements for conventional purification of diluted HCOO⁻ products would cancel the expected benefits of the CO₂ electrovalorization in terms of global warming footprint [48]. In order to electrochemically reduce CO₂ to HCOO⁻ at the industrial scale in a sustainable way, a simultaneous achievement of the previous requirements mentioned should be considered. Accordingly, obtaining noteworthy results simultaneously in terms of the product concentration, the FE for HCOO⁻ and the consumption of energy should be considered mandatory for an implementation of the electrocatalytic reduction of CO₂ to HCOO⁻ at the industrial scale.

Different research groups [31–35,38,40] have made great efforts and advances for the electrocatalytic CO₂ reduction to HCOOH or HCOO⁻ in a continuous mode. The experimental conditions and the results of these studies are summarized in Table S1 of the Supplementary Information. Some studies have recently been developed by Díaz-Sainz et al 2019 [38,40] employing carbon supported Bi nanoparticles in different working electrode configurations (Gas Diffusion Electrodes (GDEs) and Catalyst Coated Membrane Electrodes (CCMEs)). The best operating conditions were obtained using Bi carbon supported nanoparticles in the form of Catalyst Coated Membrane Electrode, in which the catalyst is deposited over the membrane Nafion 117. Hence, operating with a current density of 45 mA·cm⁻² and a Bi catalyst loading of 1.5 mg·cm⁻², noteworthy results were obtained in terms of formate concentration ([HCOO⁻]) and FE for HCOO⁻: 34 g·L⁻¹ and 72%, respectively [40]. Proietto et al 2018 [31] and Ramdin et al 2019 [32] described interesting studies of CO₂ electroreduction to HCOO⁻ at high pressure, obtaining [HCOO⁻] of 17.2 and 20 g·L⁻¹, respectively. Nevertheless, FE for HCOO⁻ obtained operating at these conditions were lower than 60 and 70%, with a pressure in the CO₂ input stream of 23 and 50 bar, respectively. Lee et al 2018 [33] studied the

electroconversion of CO_2 to HCOO^- , yielding $[\text{HCOO}^-]$ and FE of $116.2 \text{ g}\cdot\text{L}^{-1}$ and 77.7%, respectively, with low energy consumption per kmol of HCOO^- ($152 \text{ kWh}\cdot\text{kmol}^{-1}$ of HCOO^-), but using a high temperature of the electrochemical cell of 323 K. Approaches using three compartment electrochemical reactors with a cation and anion exchange membrane for the electrocatalytic reduction of CO_2 to HCOOH have been studied [34,35]. Yang et al 2017 [35] implemented an efficient CO_2 electroreduction to HCOOH , obtaining formic acid concentration ($[\text{HCOOH}]$), FE for HCOOH and consumption of energy of $94 \text{ g}\cdot\text{L}^{-1}$, 94% and $200 \text{ kWh}\cdot\text{kmol}^{-1}$ of HCOOH . Xia et al 2019 [34] achieved $[\text{HCOOH}]$ of 309 and $556 \text{ g}\cdot\text{L}^{-1}$, but at the expense of obtaining FE values of 30 and 40%, respectively, with important values of energy consumption (536 and $368 \text{ kWh}\cdot\text{kmol}^{-1}$ of HCOOH , respectively). The results of the studies mentioned above show an important progress in the electrocatalytic reduction of CO_2 to HCOOH or HCOO^- . Other recent and relevant studies have also been published [49–52]. Nevertheless, the results reported do not involve a simultaneous combination of the mandatory requirements for an implementation of the process at the industrial scale. As depicted in Fig. 1, it is required to obtain significant concentrations of the target product, but simultaneously achieving remarkable values of the FE (Fig. 1a) and of the energy consumption per kmol of the target product (Fig. 1b). Therefore, there is the need of further research efforts to reach simultaneously desirable values of the different figures of merit involved in the assessment of these processes. Here we report a process for the electrochemical reduction of CO_2 to obtain HCOO^- on a continuous mode, with only one pass of the input stream through the cell, employing Bi carbon supported nanoparticles (Bi/C NPs) in the form of a membrane electrode assembly (Bi-MEA). The input to the cathode is only CO_2 humidified and the process developed results in FE, concentration of product obtained, and energy consumption in a better trade-off than previous approaches reported in

literature. As illustrated in Fig. 1, the FE for HCOO^- and the consumption of energy per kmol of HCOO^- obtained is close to the highest value reported in the literature, but simultaneously, the $[\text{HCOO}^-]$ obtained is three times higher than these studies. It is also particularly noteworthy that the values of energy per kmol of HCOO^- required are lower than previous approaches, under current densities that allow yielding $[\text{HCOO}^-]$ higher than $300 \text{ g}\cdot\text{L}^{-1}$.

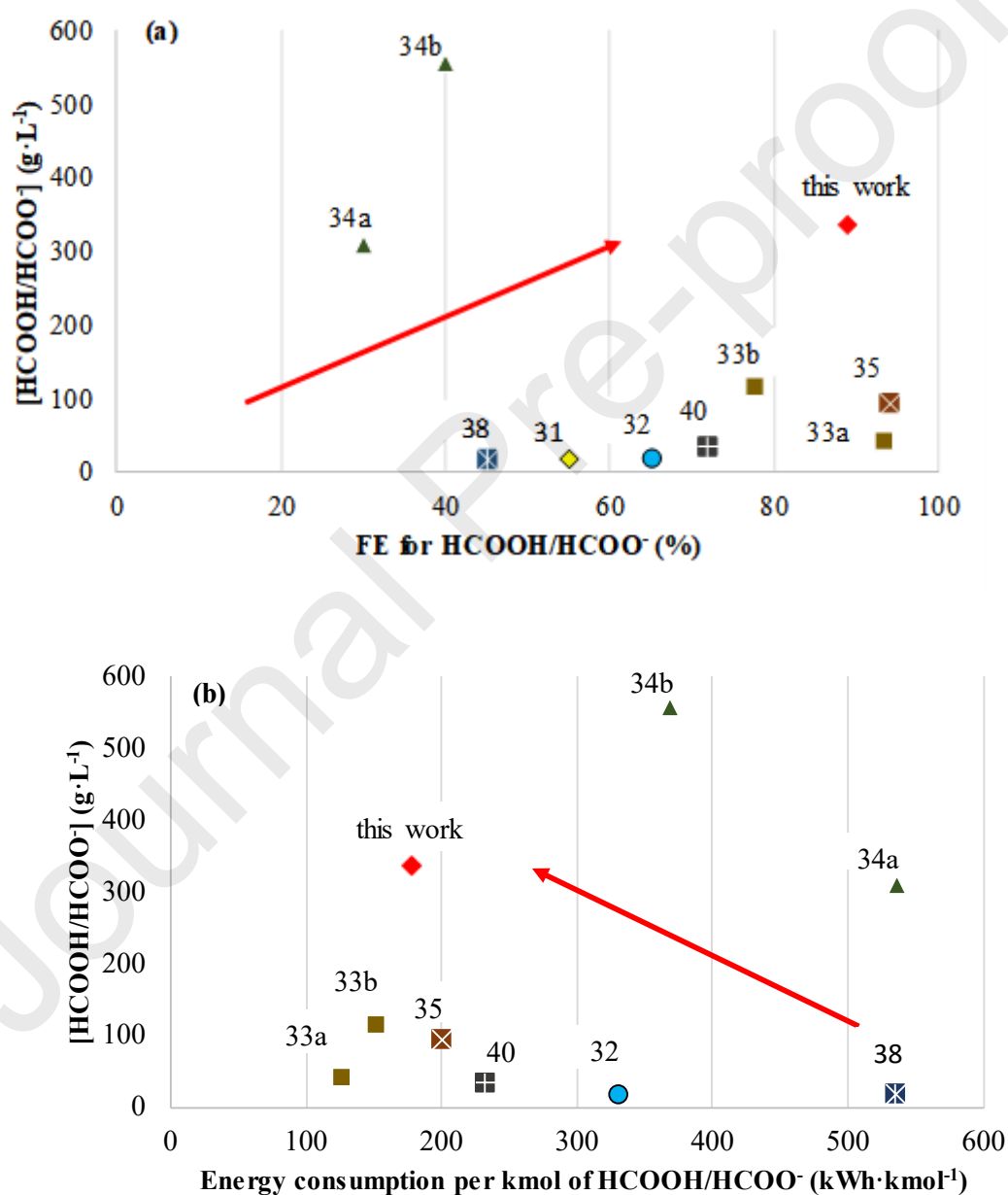


Fig. 1. State of the art for electrocatalytic reduction of CO_2 to HCOOH or HCOO^- in continuous operation. Results in terms of combination of (a) product concentration ($[\text{HCOOH}]/[\text{HCOO}^-]$) and FE for

HCOOH/HCOO⁻; (b) product concentration ([HCOOH]/[HCOO⁻]) and energy consumption per kmol of HCOOH/HCOO⁻ (31, 32, 33, 34, 35, 38 and 40). The data featured in this study are indicated in red (♦).

2. Materials and methods

2.1 Synthesis of bismuth electrocatalysts

Carbon-supported Bi nanoparticles (Bi/C NPs) were synthesized by chemical reduction of Bi³⁺, in N,N-Dimethylformamide (DMF) as solvent, by NaBH₄ in the presence of polyvinylpyrrolidone (PVP) as capping agent. This synthesis method was described in a recent contribution [53]. In more detail, 0.316 g of BiCl₃ (99.99%, Aldrich) was used as Bi precursor, 0.112 g of PVP (K30, Mw ~55.000, Aldrich) were added into 37.92 g of DMF (99.8%, Sigma Aldrich) and sonicated until complete solubilisation. Then, 0.116 g of NaBH₄ (99%, Aldrich) were added to the solution under continuous magnetic stirring at room temperature. After the addition of the reducing agent the solution becomes dark indicating the reduction of Bi³⁺ to Bi⁰. The solution was stirred and alternatively sonicated for 45 min. Subsequently, 0.836 g of carbon Vulcan XC-72R were added to the mixture to obtain a Bi loading of ca. 20 wt.%. After 60 min of continuous magnetic stirring with alternative sonication, the Bi/C nanoparticles were precipitated using acetone and filtered and washed with acetone through a nylon membrane filter of 45 mm. Finally, the sample is dried overnight under vacuum conditions at 45 °C.

2.2 Preparation of Bi-GDE and Bi-MEA

Bi-GDEs were used as cathode in the electrochemical filter press cell. The GDE is composed of three different layers: the carbonaceous support, the microporous layer and the catalytic layer, as depicted in Fig. S1. The preparation of the GDE is also described in the Supplementary Information.

The Bi-MEA consists of a cationic exchange membrane in contact with the GDE (as illustrated in Fig. S2), which acts as a separator between anode and cathode compartment

of the electrochemical reactor. Nafion 117 membrane was used as the cationic exchange membrane. Moreover, the current collector is located directly between the GDE and the cationic exchange membrane.

2.3 Characterization

Transmission electron microscopy (TEM) images were obtained with a JEOL JEM-1400 Plus working at 120 kV to evaluate the particle size and dispersion of the Bi nanoparticles. X-ray diffraction (XRD) patterns were obtained with a Bruker D8 Advance diffractometer (Bruker, Billerica, MA, USA) fitted with a copper tube. The optical setup included a Ni 0.5% CuK β filter in the secondary beam so that only CuK α radiation illuminated the sample (CuK α 1=0.154059 nm and CuK α 2=0.154445 nm). The sample was spread onto a Si wafer and measured in reflection geometry over the 20–90° 2 θ range with a step of 0.10° and a counting time of 30s per step. X-ray photoelectron spectroscopy (XPS) experiments were recorded on a K-Alpha Thermo Scientific spectrometer using AlK α 1486.6eV radiation, monochromatised by a twin crystal monochromator and yielding a focused X-ray spot with a diameter of 400 μ m, at 3mA x 12kV. Deconvolution of the XPS spectra was carried out using a Shirley background. High resolution SEM images were obtained using a field emission scanning electron microscopy (FESEM) (ZEISS model Merlin VP Compact).

The electrochemical characterization of the Bi-based electrodes was performed in a three-electrode configuration glass cell in Ar or CO₂-saturated 0.5 M KHCO₃ (99.7%, Sigma Aldrich) solution employing a platinum wire and an AgCl/Ag (3.5 M KCl) as counter and reference electrodes, respectively. Cyclic voltammetry (CV) experiments were performed using a PGSTAT302N Metrohm Autolab B. V. All CV measurements were performed at 25 \pm 1 °C.

2.4 Filter press cell configuration and experimental conditions for the electrochemical CO_2 reduction

The experimental setup and the experiments conditions are described in detail in the Supplementary Information. The core of the experimental system is a filter-press reactor, whose configuration is illustrated in Fig. 2. The filter press configuration used in this work is totally different with respect to previous studies developed in DePRO research group of University of Cantabria. The configurations used in these previous studies, are described in Supporting Information and illustrated in Fig. S4 and S5.

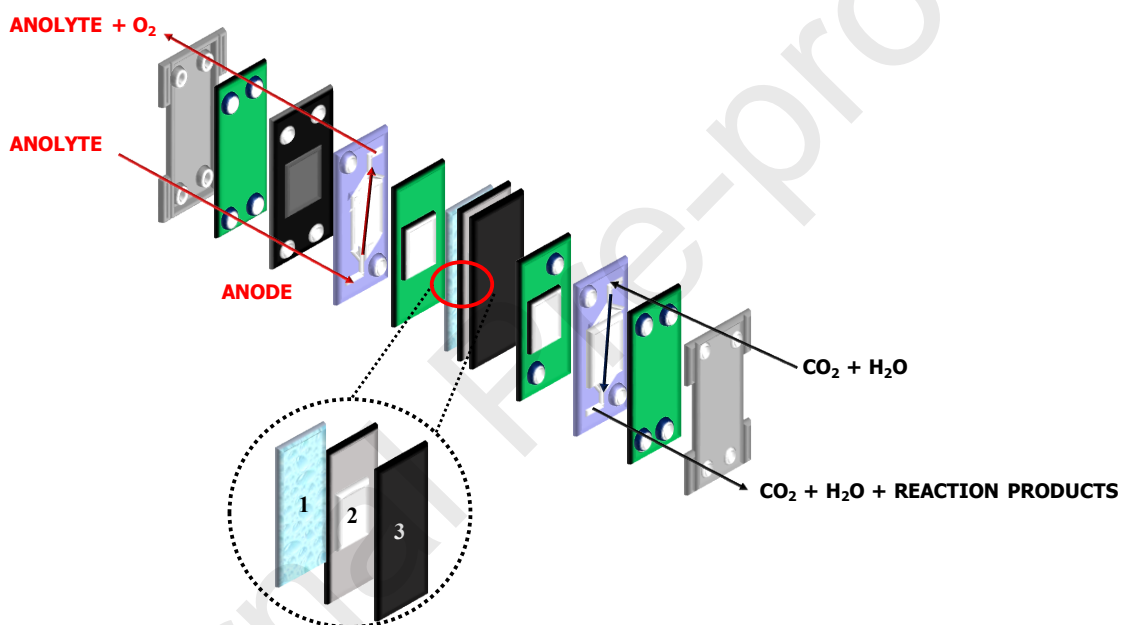


Fig. 2. Filter press scheme used for the study of the continuous electrocatalytic reduction of CO_2 to obtain HCOO^- with a single pass of the inputs through the electrochemical reactor (1: Nafion 117 membrane, 2: current collector and 3: Gas Diffusion Electrode).

The experimental system allowed continuous operation with a single pass of the reactants (which were a humidified CO_2 stream in the cathode side, and a 1 M KOH in the anode side). Both the liquid and gas output streams were analyzed. The performance of the electrochemical process is assessed by the FE, the $[\text{HCOO}^-]$, the HCOO^- rate, the energy consumption per kmol of HCOO^- and the energy efficiency. The product analysis and the

different equations used to calculate these figures of merit can be also found in the Supplementary Information.

3. Results and discussion

3.1 Characterization of the electrocatalyst (Bi/C NPs)

Fig. 3 shows the main characteristics of the Bi/C NPs used in this work. Fig. 3a displays a representative TEM image of the sample. The image shows the presence of isolated, well-dispersed and quasi-spherical Bi nanoparticles with a particle size about 9.7 ± 2.3 nm (Fig. 3b). However, it is also worth noting the presence of some Bi clusters clearly formed by aggregated Bi nanoparticles. The dimension of these aggregates is about 200-300 nm. More representative TEM images of the samples are included in the supporting information (Fig. S6).

Fig. 3c depicts the XRD patterns of the Bi/C NPs sample. Despite the fact that the diffractogram is mainly dominated by the presence of Bi oxides (Bi_2O_3), as consequence of the spontaneous oxidation during the air washing with acetone, some small contributions associated with metallic Bi with a hexagonal crystal structure can be also observed. XPS measurements were obtained to provide a more precise analysis of the surface chemical composition in relation to the oxidation states of the Bi/C NPs sample. The XPS spectrum of the Bi 4f region (Fig. 3d) shows the presence of two binding energy contributions at 164.8 (Bi 4f_{5/2}) and 159.5 eV (Bi 4f_{7/2}) [54] related to Bi³⁺. In addition, two clear shoulders are observed at 162.6 (Bi 4f_{5/2}) and 157.3 (Bi 4f_{7/2}) eV denoting the presence of Bi⁰. The Bi³⁺: Bi⁰ ratio was found to be about 94:6, confirming that the Bi/C NPs present an oxidized character.

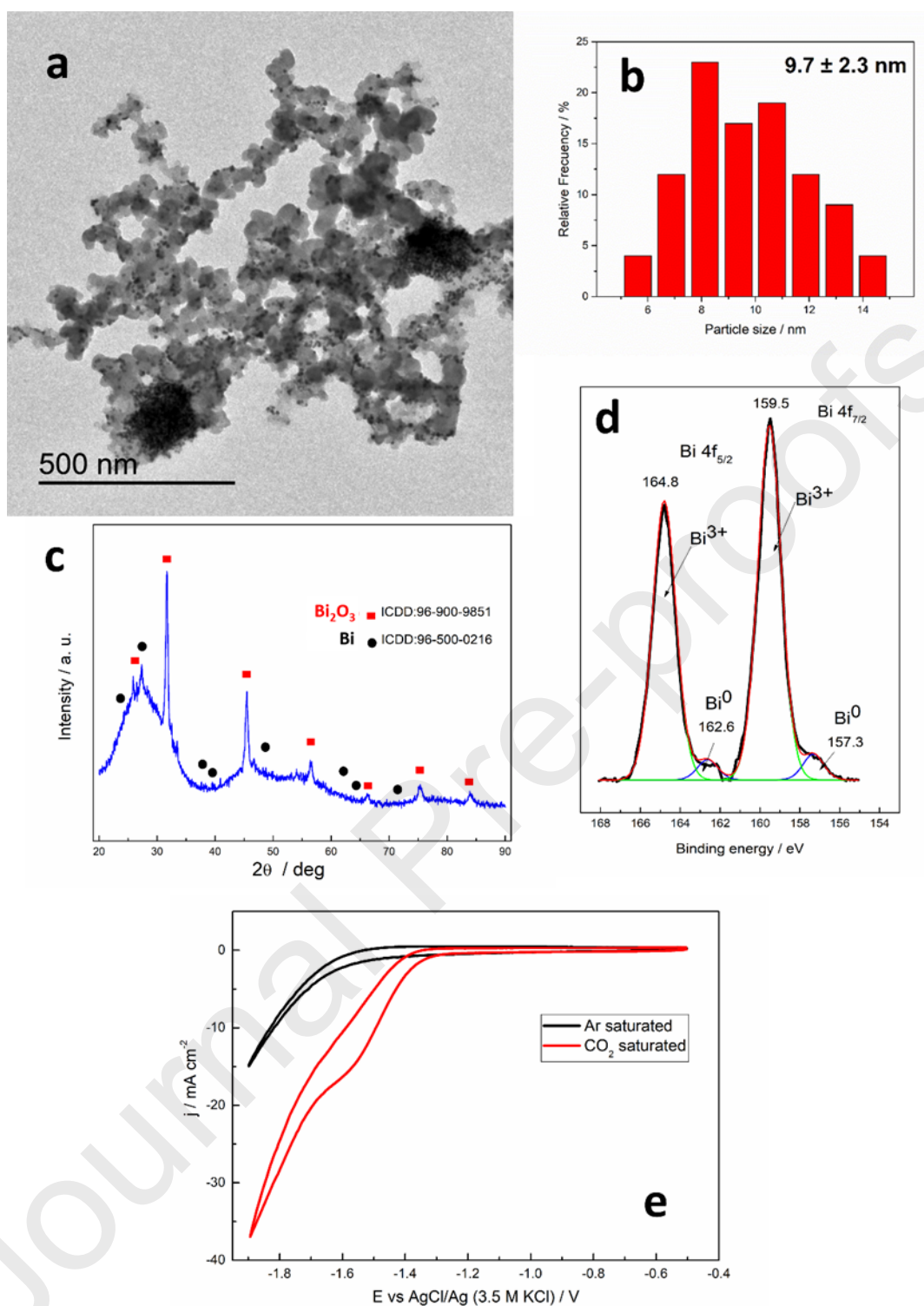


Fig. 3. (a) Representative TEM image of the Bi/C NPs, and (b) the corresponding particle size histogram. (c) XRD diffractogram of the Bi/C NPs. (d) High resolution XPS spectra recorded of Bi 4f region of the Bi/C NPs and (e) Cyclic voltammetry response of Bi/C electrode with Bi loading of $0.1 \text{ mg} \cdot \text{cm}^{-2}$ in Ar (black line) and CO_2 (red line) saturated 0.5 M KHCO_3 . Scan rate 50 mV s^{-1} .

To complete this characterization of the material, Fig. 3e displays the electrochemical response of a Bi/C NPs electrode in an Ar and CO₂ saturated 0.5 M KHCO₃ solution. In the Ar saturated solution, the voltammogram shows a reduction process due to the hydrogen evolution reaction (HER) which appears at about -1.4 V vs AgCl/Ag. For the CO₂ saturated solution, the results obtained clearly display the presence of a new and well-defined reduction process, starting at -1.3 V, and associated with the CO₂ reduction.

3.2 Characterization of the electrodes (Bi/C-GDEs).

The Bi/C GDEs were also characterized (surface and cross section) by SEM/EDX. Fig. 4 reports some representative SEM images obtained using backscattered electrons. As previously shown in the TEM images, the SEM images of the surface of the electrodes (Fig. 4a and 4c) show both well-isolated and aggregated Bi nanoparticles. As expected, the surface of both electrodes is essentially similar independently of the metal loading (0.75 (a) and 1.5 (b) mg Bi/C NPs·cm⁻²). However, the cross section SEM images of the electrodes show that the thickness of the catalytic layer (CL) increases for increasing metal loading (Fig. 4b and 4d). Thus, for 0.75 mg Bi/C NPs·cm⁻², the thickness of the CL is about 80 μm, while, for 1.5 mg Bi/C NPs·, the thickness of the CL is about 150 μm. This different thickness may play an important role during the gas-phase CO₂ electroreduction experiments. In this context, this thickness directly affects the ohmic resistance of the electrochemical reactor, increasing the cathode potential achieved operating with a Bi catalyst loading of 1.5 mg·cm⁻² with respect to the employ of Bi-based electrodes with a loading of 0.75 mg·cm⁻².

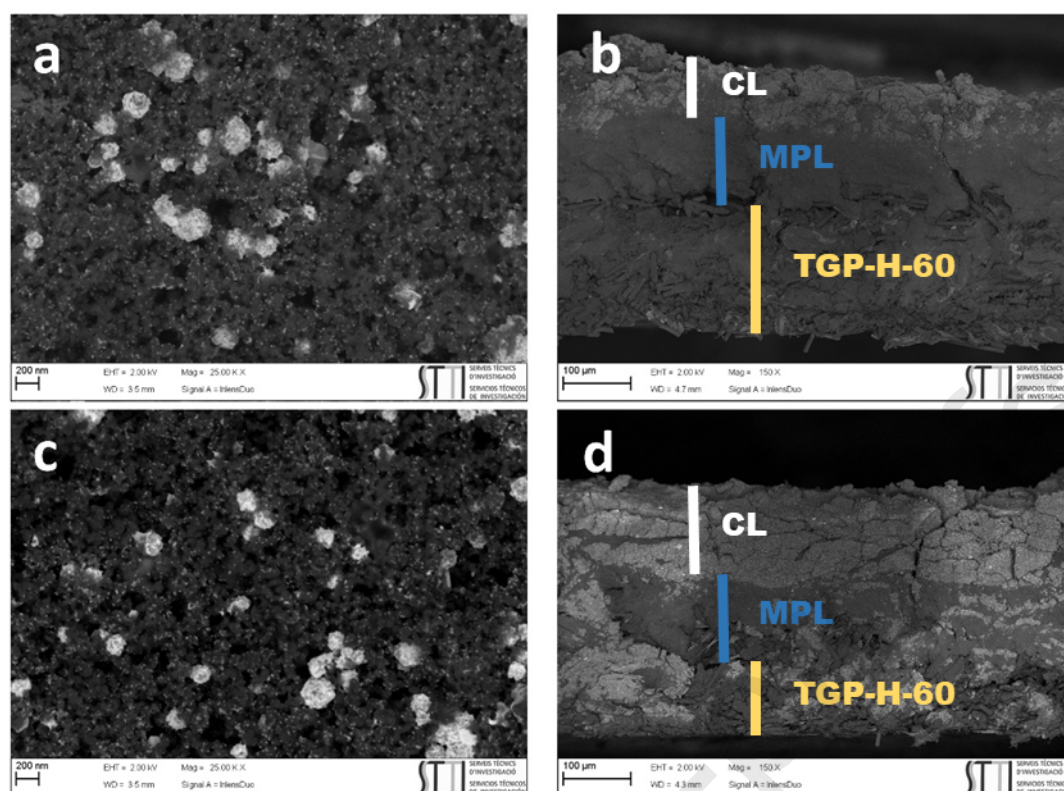


Fig. 4. SEM images of the Bi-GDEs, (a, c) surface and (b, d) cross section. Back-scattered electrons field emission SEM images of the Bi-based electrodes with Bi loading of $0.75 \text{ mg}\cdot\text{cm}^{-2}$ (a, b) and $1.5 \text{ mg}\cdot\text{cm}^{-2}$ (c, d).

3.3 Performance of the electrochemical continuous process.

Various experiments were carried out at room temperature ($20 \text{ }^{\circ}\text{C}$) to analyze the performance of the process operating at different current densities and water flows in the input stream to the electrochemical filter press cell. All the tests were done working in a continuous mode with only one pass of the inputs through the filter press cell. Moreover, similar experiments were conducted at different Bi catalyst load: $0.75 \text{ mg}\cdot\text{cm}^{-2}$ and $1.5 \text{ mg}\cdot\text{cm}^{-2}$. The detailed results of this section, as well as the potentials measured at the different tests are reported in Tables S2, S3, S4 and S5 of the Supplementary Information.

3.3.1 Filter press tests with a Bi catalyst load of $0.75 \text{ mg}\cdot\text{cm}^{-2}$

Different current densities and water flows in the CO_2 input stream with an amount of Bi catalyst of $0.75 \text{ mg}\cdot\text{cm}^{-2}$ were tested. The results of these experiments are graphically

summarized and compared in Fig. 5 and 6 (values are reported in Table S2). On the one hand, as shown in Fig. 5, operating with the same value of the water flow ($0.5 \text{ g}\cdot\text{h}^{-1}$), a rise of the current density from 45 to $100 \text{ mA}\cdot\text{cm}^{-2}$ results in a significant increment of $[\text{HCOO}^-]$ from 201 to $256 \text{ g}\cdot\text{L}^{-1}$, approximately 27 per cent. Notwithstanding, as expected, the FE for HCOO^- declined by roughly half, from 71 to 41%. In contrast, although supplying the filter press reactor with a current density of $200 \text{ mA}\cdot\text{cm}^{-2}$ results in one of the highest values of $[\text{HCOO}^-]$ reported in literature ($312 \text{ g}\cdot\text{L}^{-1}$), the FE for HCOO^- is still far from a desirable value for an implementation of the process at the industrial scale (25%). This decrease in the FE for HCOO^- can be explained by the increment of the hydrogen (H_2) production by the hydrogen evolution reaction (HER). Thus, the FE for H_2 raised from 22 to 69% when the current density was increased from 45 to $200 \text{ mA}\cdot\text{cm}^{-2}$ (FE for H_2 values are reported in the Table S3).

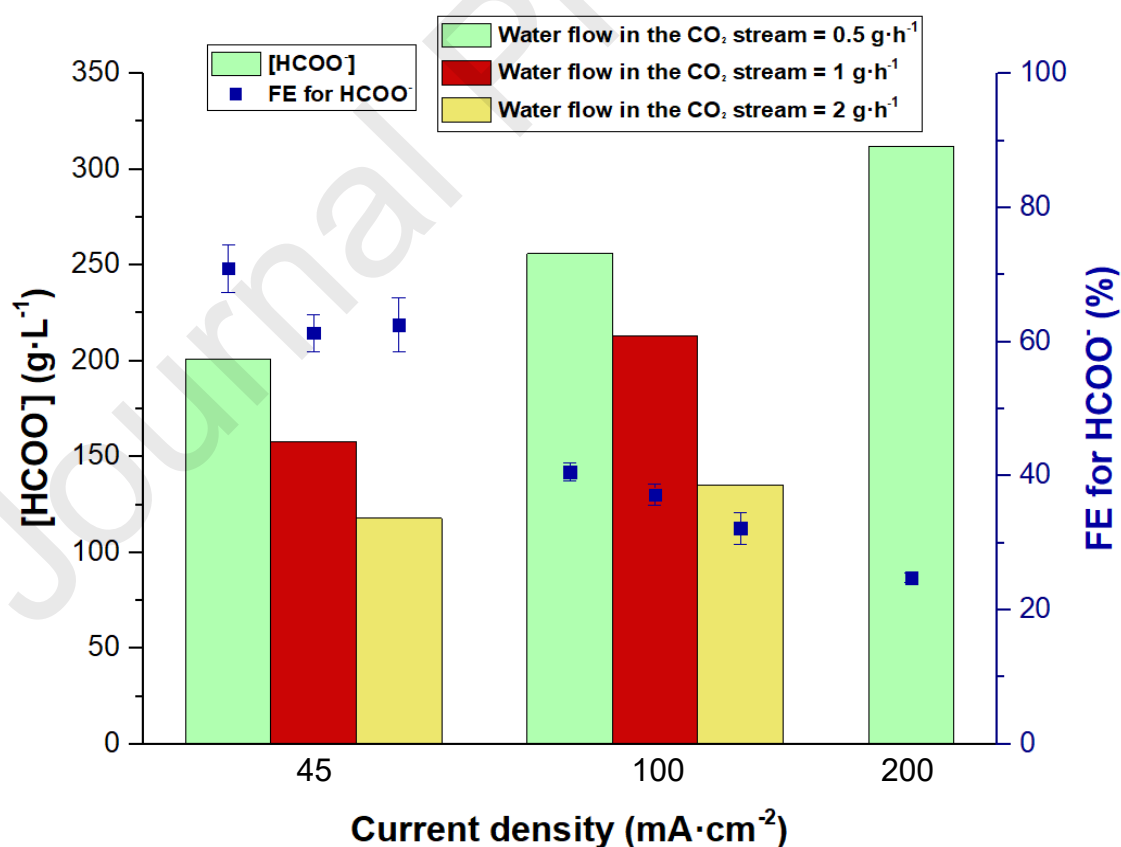


Fig. 5. Performance of the electrocatalytic reduction of CO₂ to HCOO⁻ employing a Bi catalyst loading of 0.75 mg·cm⁻² in terms of HCOO⁻ concentration (g·L⁻¹) and Faradaic efficiency for HCOO⁻ (%) as a function of the current density (mA·cm⁻²) and the water flow in the CO₂ input stream (g·h⁻¹).

Additional tests were done at the same current densities (45 and 100 mA·cm⁻²), but at different water flows in the CO₂ stream (1 and 2 g·h⁻¹). In both cases, the same phenomena were observed when the water flow was increased from 0.5 to 2 g·h⁻¹. The [HCOO⁻] sharply decreased to 118 and 135 g·L⁻¹ and simultaneously, FE for HCOO⁻ also decreased to 62.5 and 32.2%, working at a current density of 45 and 100 mA·cm⁻², respectively, as can be seen in Fig. 5. We hypothesized that this simultaneous decrease in the [HCOO⁻] and the FE for HCOO⁻ is because increasing the amount of water vapor supplied to the electrochemical reactor results in a significant dilution of the HCOO⁻ obtained by electroreduction of CO₂, and simultaneously the excess of water vapor supplied favors the HER., decreasing the FE for HCOO⁻.

Furthermore, the energy consumption per kmol of HCOO⁻ was only 207.7 kWh·kmol⁻¹ of HCOO⁻, which corresponds to an absolute cell potential of 2.75 V, operating with a current density and a water flow of 45 mA·cm⁻² and 0.5 g·h⁻¹, respectively. As displayed in Fig. 6, increasing the current density and the water flow in the CO₂ stream, the performance of the electrochemical filter press in terms of energy consumption per kmol of HCOO⁻ got worse. Such results are found to be caused by higher ohmic and mass transfer losses imposed by the higher current density and water flow in the CO₂ stream. However, the increase of the current density supplied to the electrochemical reactor, when the water flow remained constant, favored the production of HCOO⁻.

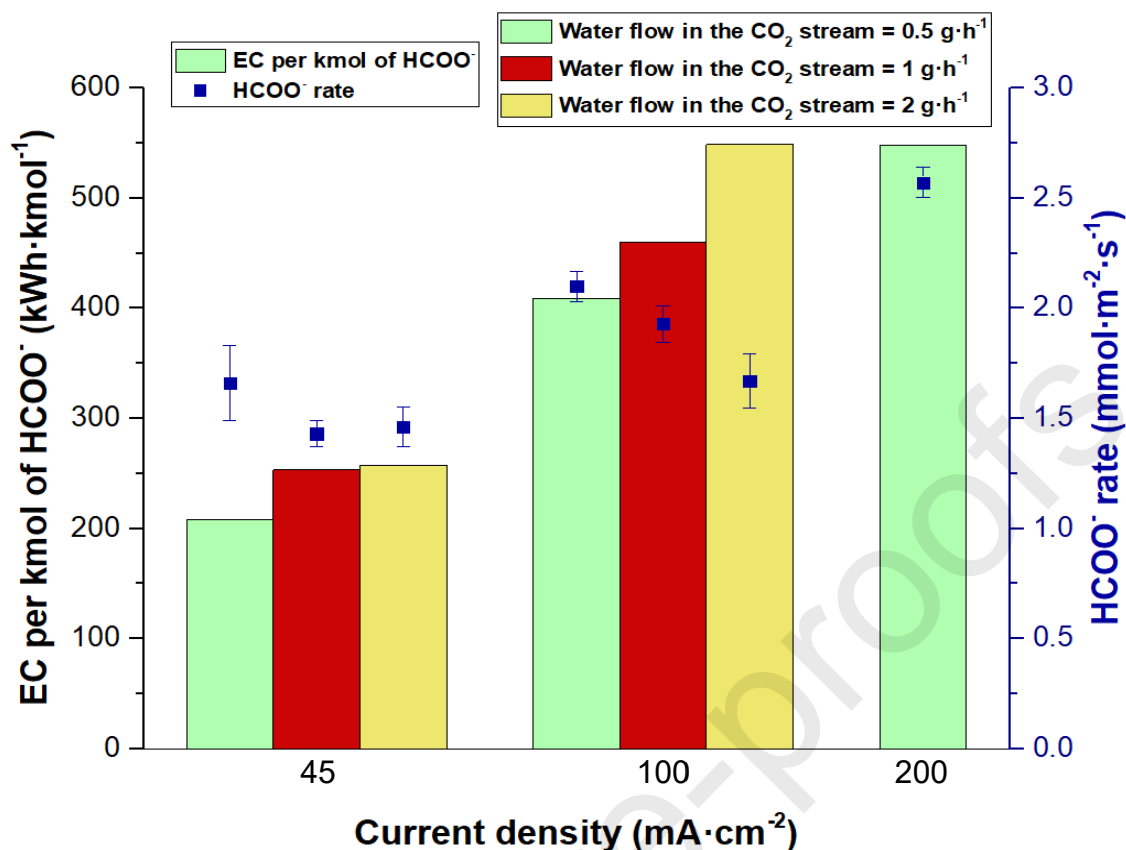


Fig. 6. Performance of the electrocatalytic reduction of CO₂ to HCOO⁻ employing a Bi catalyst loading of 0.75 mg·cm⁻² in terms of energy consumption per kmol of HCOO⁻ (kWh·kmol⁻¹) and HCOO⁻ rate (mmol·m⁻²·s⁻¹) as a function of the current density (mA·cm⁻²) and the water flow in the CO₂ input stream (g·h⁻¹).

3.3.2 Filter press tests with a Bi catalyst load of 1.5 mg·cm⁻²

Additional experiments were performed with a Bi catalyst loading of 1.5 mg·cm⁻² in the working electrode of the electrochemical filter press. The current densities supplied to the electrochemical cell were the same as those employing 0.75 mg·cm⁻², with the exception of operating at 200 mA·cm⁻² due to the low FE for HCOO⁻ value obtained in the previous experiments. The results obtained are graphically summarized and compared in Fig. 7 and 8 (values are provided in Table S4).

As shown in Fig. 7, the performance of the process under 100 mA·cm⁻² follows the same trends observed in the previous experiments (Fig. 5): an increase of the input water flow results in a decrease in [HCOO⁻] and in FE for HCOO⁻. This can also be attributed to a

dilution effect, as well as to a promotion of HER revealed by the increase of the FE for H_2 with water flow at $100 \text{ mA}\cdot\text{cm}^{-2}$ reported in Table S5. A high concentration (approx. $340 \text{ g}\cdot\text{L}^{-1}$) can be obtained at $100 \text{ mA}\cdot\text{cm}^{-2}$ with a water flow of $0.5 \text{ g}\cdot\text{h}^{-1}$, but achieving a FE for HCOO^- of only 41%.

The performance of the process is clearly improved operating at $45 \text{ mA}\cdot\text{cm}^{-2}$. It is noteworthy that, working at this current density, an optimum input water flow is found at $2 \text{ g}\cdot\text{h}^{-1}$ (Fig. 7), which allowed yielding a $[\text{HCOO}^-]$ of $337 \text{ g}\cdot\text{L}^{-1}$ with an excellent FE for HCOO^- of 89%. To the best of our knowledge, under these operating conditions resulted in the best trade-off between $[\text{HCOO}^-]$ and FE for HCOO^- reported in the literature.

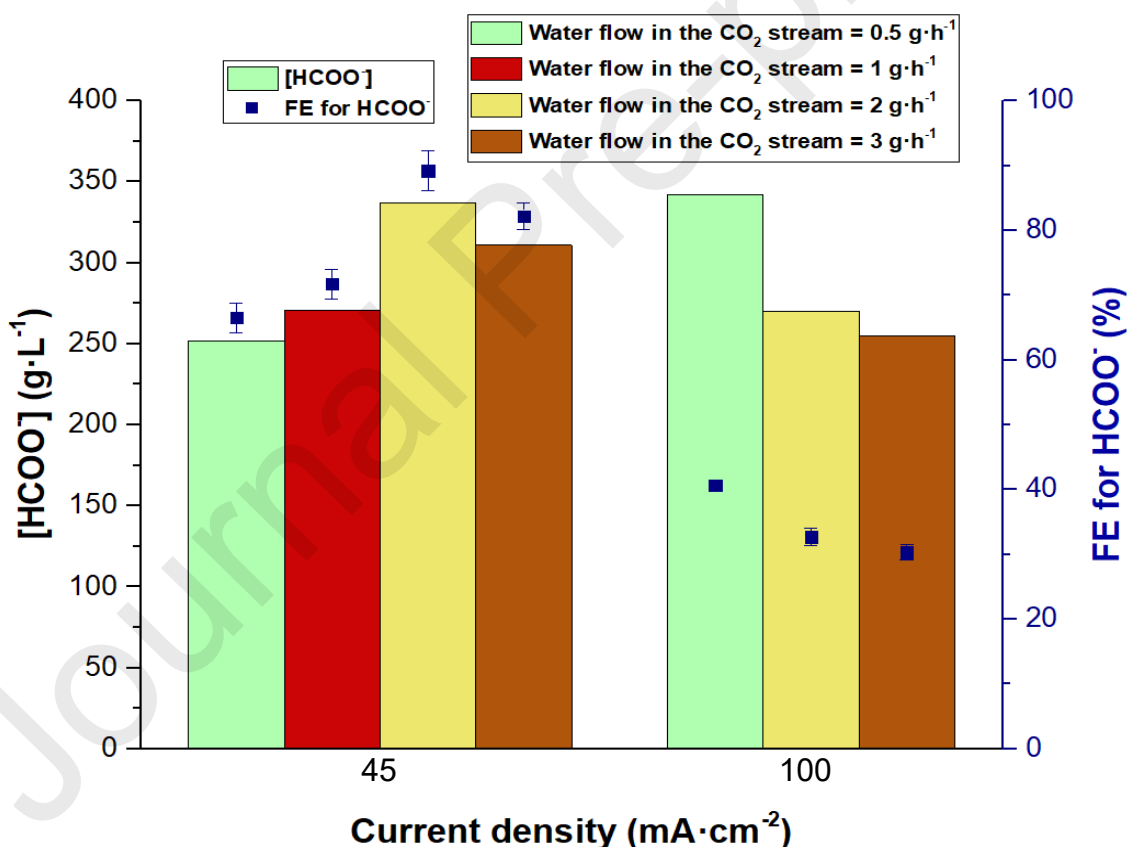


Fig. 7. Performance of the electrocatalytic reduction of CO_2 to HCOO^- employing a Bi catalyst loading of $1.5 \text{ mg}\cdot\text{cm}^{-2}$ in terms of HCOO^- concentration ($\text{g}\cdot\text{L}^{-1}$) and Faradaic efficiency for HCOO^- (%) as a function of the current density ($\text{mA}\cdot\text{cm}^{-2}$) and the water flow in the CO_2 input stream ($\text{g}\cdot\text{h}^{-1}$).

In terms of energy consumption, as depicted in Fig. 8, supplying a current density of $45 \text{ mA}\cdot\text{cm}^{-2}$ and a water flow of $2 \text{ g}\cdot\text{h}^{-1}$, the energy consumption per kmol of HCOO^- was only of $180 \text{ kWh}\cdot\text{kmol}^{-1}$, which corresponds to an energy efficiency and an absolute cell potential of 56.1% and 3 V, respectively. Moreover, increasing the current density results in a higher energy consumption per kmol of HCOO^- , similarly as reported employing $0.75 \text{ mg}\cdot\text{cm}^{-2}$, operating with the same water flow in the CO_2 stream.

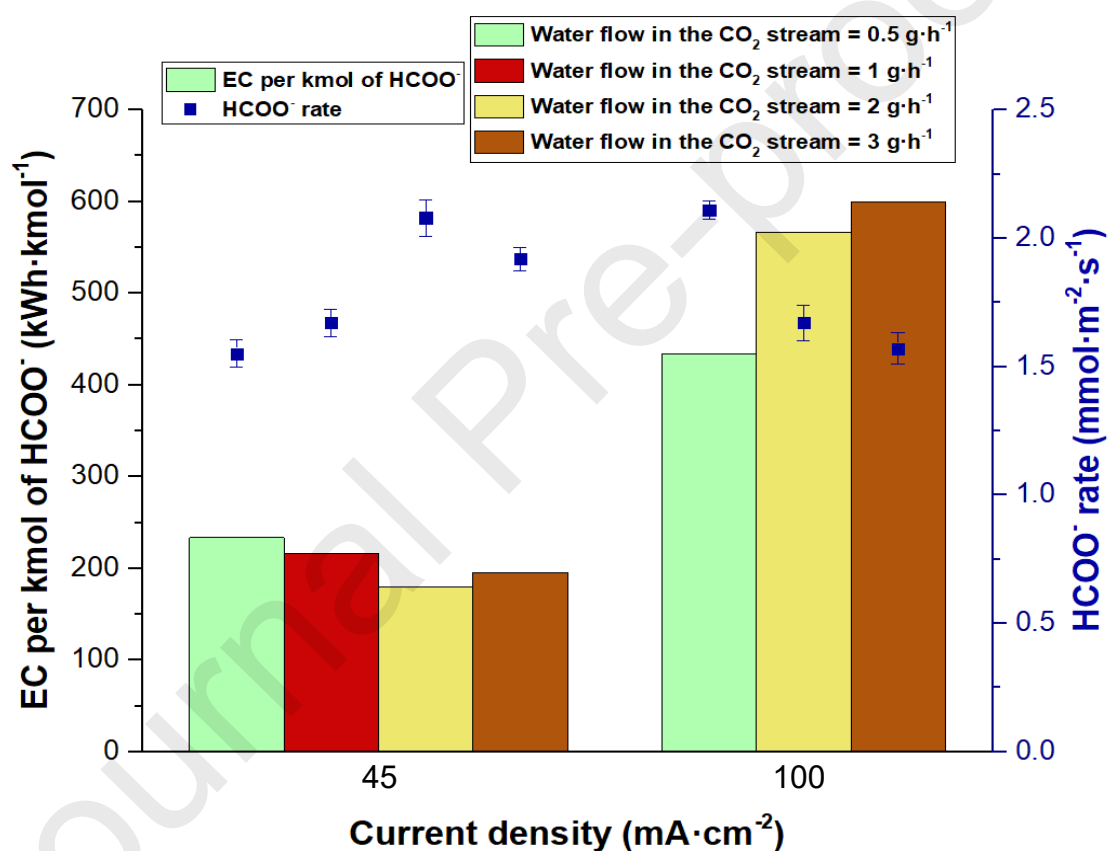


Fig. 8. Performance of the electrocatalytic reduction of CO_2 to HCOO^- employing a Bi catalyst loading of $1.5 \text{ mg}\cdot\text{cm}^{-2}$ in terms of energy consumption per kmol of HCOO^- ($\text{kWh}\cdot\text{kmol}^{-1}$) and HCOO^- rate ($\text{mmol}\cdot\text{m}^{-2}\cdot\text{s}^{-1}$) as a function of the current density ($\text{mA}\cdot\text{cm}^{-2}$) and the water flow in the CO_2 input stream ($\text{g}\cdot\text{h}^{-1}$).

As demonstrated in Fig. 1, this remarkable consumption of energy ($180 \text{ kWh}\cdot\text{kmol}^{-1}$) represents an important progress in the electrocatalytic reduction of CO_2 to HCOO^- due to the trade-off between the $[\text{HCOO}^-]$ ($337 \text{ g}\cdot\text{L}^{-1}$), the FE for HCOO^- (89%) and the

energy consumption per kmol of HCOO^- , important requirements for a future implementation of the process at the industrial scale.

4. Conclusions

In this study, an important progress for the electrocatalytic reduction of CO_2 to HCOO^- has been obtained. A process for the continuous electroreduction of CO_2 to HCOO^- in a continuous mode with a single pass of the inputs through the electrochemical filter press cell has been developed. The working electrodes were prepared by depositing the Bi carbon supported nanoparticles in the form of Gas Diffusion Electrodes. However, the mass transfer between the working electrode and the Nafion 117 membrane was improved due to the direct contact between these elements of the filter press cell.

The improvement of the mass transfer of the electrochemical filter press results in remarkable results in terms of $[\text{HCOO}^-]$, FE for HCOO^- and the consumption of energy per kmol of HCOO^- of $337 \text{ g}\cdot\text{L}^{-1}$, 89% and $180 \text{ kWh}\cdot\text{kmol}^{-1}$, respectively. These results represent the best trade-off in these figures of merit reported in the literature. Moreover, these results were obtained operating in a continuous mode and at a current density, a water flow in the CO_2 stream and a Bi catalyst loading of $45 \text{ mA}\cdot\text{cm}^{-2}$, $2 \text{ g}\cdot\text{h}^{-1}$ and $1.5 \text{ mg}\cdot\text{cm}^{-2}$, respectively, at ambient conditions of temperature and pressure.

Hence, this configuration of the electrochemical filter press reactor has improved the performance of the electrocatalytic reduction of CO_2 to HCOO^- and it makes the electrochemical process closer to the future implementation at the industrial scale.

Acknowledgments

The authors of this work would like to acknowledge to the financial support from the MINECO, through the projects CTQ2016-76231-C2-1-R and CTQ2016-76231-C2-2-R

(AEI/FEDER, UE). J.S.G acknowledges financial support from VITC (Vicerrectorado de Investigación y Transferencia de Conocimiento) of the University of Alicante (UTALENTO16-02). G.D.S, M.A.G and A.I filed a patent application on the experimental reaction system discussed here.

Declaration of Competing Interest

The authors declare no conflict of interest.

References

- [1] B. Endródi, G. Bencsik, F. Darvas, R. Jones, K. Rajeshwar, C. Janáky, Continuous-flow electroreduction of carbon dioxide, *Prog. Energy Combust. Sci.* 62 (2017) 133–154. doi:10.1016/j.pecs.2017.05.005.
- [2] J. Qiao, Y. Liu, J. Zhan, *Electrochemical Reduction of Carbon Dioxide. Fundamentals and Technologies*, CRC Press, Boca Raton, 2016.
- [3] A.J. Martín, G.O. Larrazábal, J. Pérez-Ramírez, Towards sustainable fuels and chemicals through the electrochemical reduction of CO₂: lessons from water electrolysis, *Green Chem.* 17 (2015) 5114–5130. doi:10.1039/C5GC01893E.
- [4] W. Zhang, Y. Hu, L. Ma, G. Zhu, Y. Wang, X. Xue, R. Chen, S. Yang, Z. Jin, Progress and Perspective of Electrocatalytic CO₂ Reduction for Renewable Carbonaceous Fuels and Chemicals, *Adv. Sci.* 5 (2018) 1700275. doi:10.1002/advs.201700275.
- [5] P.R. Yaashikaa, P. Senthil Kumar, S.J. Varjani, A. Saravanan, A review on photochemical, biochemical and electrochemical transformation of CO₂ into value-added products, *J. CO₂ Util.* 33 (2019) 131–

- 147.doi:10.1016/j.jcou.2019.05.017.
- [6] F.P. García de Arquer, C.T. Dinh, A. Ozden, J. Wicks, C. McCallum, A.R. Kirmani, D.H. Nam, C. Gabardo, A. Seifitokaldani, X. Wang, Y.C. Li, F. Li, J. Edwards, L.J. Richter, S.J. Thorpe, D. Sinton, E.H. Sargent, CO₂ electrolysis to multicarbon products at activities greater than 1 A cm⁻², *Science* 367 (2020) 661–666. doi:10.1126/science.aay4217.
- [7] I. Merino-Garcia, E. Alvarez-Guerra, J. Albo, A. Irabien, Electrochemical membrane reactors for the utilisation of carbon dioxide, *Chem. Eng. J.* 305 (2016) 104–120. doi:10.1016/j.cej.2016.05.032.
- [8] Y. Yang, M. Wu, X. Zhu, H. Xu, S. Ma, Y. Zhi, H. Xia, X. Liu, J. Pan, J.Y. Tang, S.P. Chai, L. Palmisano, F. Parrino, J. Liu, J. Ma, Z.L. Wang, L. Tan, Y.F. Zhao, Y.F. Song, P. Singh, P. Raizada, D. Jiang, D. Li, R.A. Geioushy, J. Ma, J. Zhang, S. Hu, R. Feng, G. Liu, M. Liu, Z. Li, M. Shao, N. Li, J. Peng, W.J. Ong, N. Kornienko, Z. Xing, X. Fan, J. Ma, 2020 Roadmap on two-dimensional nanomaterials for environmental catalysis, *Chinese Chem. Lett.* 30 (2019) 2065–2088. doi:10.1016/j.ccllet.2019.11.001.
- [9] Z. Wei, B. Ding, H. Dou, J. Gascon, X.J. Kong, Y. Xiong, B. Cai, R. Zhang, Y. Zhou, M. Long, J. Miao, Y. Dou, D. Yuan, J. Ma, 2020 Roadmap on Pore Materials for Energy and Environmental Applications, *Chinese Chem. Lett.* 30 (2019) 2110–2122. doi:10.1016/j.ccllet.2019.11.022.
- [10] S. Verma, B. Kim, H.R.M. Jhong, S. Ma, P.J.A. Kenis, A gross-margin model for defining technoeconomic benchmarks in the electroreduction of CO₂, *ChemSusChem.* 9 (2016) 1972–1979. doi:10.1002/cssc.201600394.
- [11] A. Irabien, M. Alvarez-Guerra, J. Albo, A. Dominguez-Ramos, Electrochemical

- Conversion of CO₂ to Value-Added Products, in: C. A. Martínez-Huitle, M. A. Rodrigo, O. Scialdone (Eds.), *Electrochemical Water Wastewater Treatment*, Elsevier, 2018, pp. 29–59.
- [12] D. Du, R. Lan, J. Humphreys, S. Tao, Progress in inorganic cathode catalysts for electrochemical conversion of carbon dioxide into formate or formic acid, *J. Appl. Electrochem.* 47 (2017) 661–678. doi:10.1007/s10800-017-1078-x.
- [13] D.A. Bulushev, J.R.H. Ross, Towards Sustainable Production of Formic Acid, *ChemSusChem.* 11 (2018) 821–836. doi:10.1002/cssc.201702075.
- [14] J. Eppinger, K.W. Huang, Formic Acid as a Hydrogen Energy Carrier, *ACS Energy Lett.* 2 (2017) 188–195. doi:10.1021/acseenergylett.6b00574.
- [15] L. An, R. Chen, Direct formate fuel cells: A review, *J. Power Sources.* 320 (2016) 127–139. doi:10.1016/j.jpowsour.2016.04.082.
- [16] P. Preuster, J. Albert, Biogenic Formic Acid as a Green Hydrogen Carrier, *Energy Technol.* 6 (2018) 501–509. doi:10.1002/ente.201700572.
- [17] J.B. Vennekoetter, R. Sengpiel, M. Wessling, Beyond the catalyst: How electrode and reactor design determine the product spectrum during electrochemical CO₂ reduction, *Chem. Eng. J.* 364 (2019) 89–101. doi:10.1016/j.cej.2019.01.045.
- [18] S. Kim, W.J. Dong, S. Gim, W. Sohn, J.Y. Park, C.J. Yoo, H.W. Jang, J.L. Lee, Shape-controlled bismuth nanoflakes as highly selective catalysts for electrochemical carbon dioxide reduction to formate, *Nano Energy.* 39 (2017) 44–52. doi:10.1016/j.nanoen.2017.05.065.
- [19] X. Zhang, T. Lei, Y. Liu, J. Qiao, Enhancing CO₂ electrolysis to formate on facilely synthesized Bi catalysts at low overpotential, *Appl. Catal. B Environ.* 218 (2017)

- 46–50. doi:10.1016/j.apcatb.2017.06.032.
- [20] X. Zhang, X. Sun, S.-X. Guo, A.M. Bond, J. Zhang, Formation of lattice-dislocated bismuth nanowires on copper foam for enhanced electrocatalytic CO₂ reduction at low overpotential, *Energy Environ. Sci.* 12 (2019) 1334–1340. doi:10.1039/c9ee00018f.
- [21] K. Natsui, H. Iwakawa, N. Ikemiya, K. Nakata, Y. Einaga, Stable and Highly Efficient Electrochemical Production of Formic Acid from Carbon Dioxide Using Diamond Electrodes, *Angew. Chemie - Int. Ed.* 57 (2018) 2639–2643. doi:10.1002/anie.201712271.
- [22] Y. Fu, Y. Li, X. Zhang, Y. Liu, J. Qiao, J. Zhang, D.P. Wilkinson, Novel hierarchical SnO₂ microsphere catalyst coated on gas diffusion electrode for enhancing energy efficiency of CO₂ reduction to formate fuel, *Appl. Energy.* 175 (2016) 536–544. doi:10.1016/j.apenergy.2016.03.115.
- [23] X. Zheng, Y. Ji, J. Tang, J. Wang, B. Liu, H.G. Steinrück, K. Lim, Y. Li, M.F. Toney, K. Chan, Y. Cui, Theory-guided Sn/Cu alloying for efficient CO₂ electroreduction at low overpotentials, *Nat. Catal.* 2 (2019) 55–61. doi:10.1038/s41929-018-0200-8.
- [24] B. De Mot, J. Hereijgers, M. Duarte, T. Breugelmans, Influence of flow and pressure distribution inside a gas diffusion electrode on the performance of a flow-by CO₂ electrolyzer, *Chem. Eng. J.* 378 (2019) 122224. doi:10.1016/j.cej.2019.122224.
- [25] A. Del Castillo, M. Alvarez-Guerra, J. Solla-Gullón, A. Sáez, V. Montiel, A. Irabien, Electrocatalytic reduction of CO₂ to formate using particulate Sn electrodes: Effect of metal loading and particle size, *Appl. Energy.* 157 (2015) 165–

173. doi:10.1016/j.apenergy.2015.08.012.
- [26] Y. Zhang, W. Zhang, Y. Feng, J. Ma, Promoted CO₂ electroreduction over indium-doped SnP₃: A computational study, *J. Energy Chem.* 48 (2020) 1–6. doi:10.1016/j.jechem.2019.12.025.
- [27] F. Yang, A.O. Elnabawy, R. Schimmenti, P. Song, J. Wang, Z. Peng, S. Yao, R. Deng, S. Song, Y. Lin, M. Mavrikakis, W. Xu, Bismuthene for highly efficient carbon dioxide electroreduction reaction, *Nat. Commun.* 11 (2020) 1088. doi:10.1038/s41467-020-14914-9.
- [28] D. Wu, G. Huo, W.Y. Chen, X.Z. Fu, J.L. Luo, Boosting formate production at high current density from CO₂ electroreduction on defect-rich hierarchical mesoporous Bi/Bi₂O₃ junction nanosheets, *Appl. Catal. B Environ.* 271 (2020) 118957. doi:10.1016/j.apcatb.2020.118957.
- [29] P. Deng, F. Yang, Z. Wang, S. Chen, Y. Zhou, S. Zaman, B.Y. Xia, Metal–Organic Framework-Derived Carbon Nanorods Encapsulating Bismuth Oxides for Rapid and Selective CO₂ Electroreduction to Formate, *Angew. Chemie - Int. Ed.* 59 (2020) 10807–10813. doi:10.1002/anie.202000657.
- [30] R. Lin, J. Guo, X. Li, P. Patel, A. Seifitokaldani, Electrochemical Reactors for CO₂ Conversion, *Catalysts* 10 (2020) 473. doi.org/10.3390/catal10050473.
- [31] F. Proietto, B. Schiavo, A. Galia, O. Scialdone, Electrochemical conversion of CO₂ to HCOOH at tin cathode in a pressurized undivided filter-press cell, *Electrochim. Acta.* 277 (2018) 30–40. doi:10.1016/j.electacta.2018.04.159.
- [32] M. Ramdin, A.R.T. Morrison, M. De Groen, R. Van Haperen, R. De Kler, L.J.P. Van Den Broeke, J.P. Martin Trusler, W. De Jong, T.J.H. Vlugt, High Pressure

- Electrochemical Reduction of CO₂ to Formic Acid/Formate: A Comparison between Bipolar Membranes and Cation Exchange Membranes, *Ind. Eng. Chem. Res.* 58 (2019) 1834–1847. doi:10.1021/acs.iecr.8b04944.
- [33] W. Lee, Y.E. Kim, M.H. Youn, S.K. Jeong, K.T. Park, Catholyte-Free Electrocatalytic CO₂ Reduction to Formate, *Angew. Chemie - Int. Ed.* 57 (2018) 6883–6887. doi:10.1002/anie.201803501.
- [34] C. Xia, P. Zhu, Q. Jiang, Y. Pan, W. Liang, E. Stavitsk, Continuous production of pure liquid fuel solutions via electrocatalytic CO₂ reduction using solid-electrolyte devices, *Nat. Energy.* 4 (2019) 776-785.
- [35] H. Yang, J.J. Kaczur, S.D. Sajjad, R.I. Masel, Electrochemical conversion of CO₂ to formic acid utilizing Sustainion™ membranes, *J. CO₂ Util.* 20 (2017) 208-217. doi:10.1016/j.jcou.2017.04.011.
- [36] A. Del Castillo, M. Alvarez-Guerra, J. Solla-Gullón, A. Sáez, V. Montiel, A. Irabien, Sn nanoparticles on gas diffusion electrodes: Synthesis, characterization and use for continuous CO₂ electroreduction to formate, *J. CO₂ Util.* 18 (2017) 222–228. doi:10.1016/j.jcou.2017.01.021.
- [37] G. Díaz-Sainz, M. Alvarez-Guerra, J. Solla-Gullón, L. García-Cruz, V. Montiel, A. Irabien, Catalyst coated membrane electrodes for the gas phase CO₂ electroreduction to formate, *Catal. Today.* 346 (2020) 58-64. doi:10.1016/j.cattod.2018.11.073.
- [38] G. Díaz-Sainz, M. Alvarez-Guerra, J. Solla-Gullón, L. García-Cruz, V. Montiel, A. Irabien, CO₂ electroreduction to formate: Continuous single-pass operation in a filter-press reactor at high current densities using Bi gas diffusion electrodes, *J. CO₂ Util.* 34 (2019) 12–19. doi:10.1016/j.jcou.2019.05.035.

- [39] D. Kopljar, A. Inan, P. Vindayer, N. Wagner, E. Klemm, Electrochemical reduction of CO₂ to formate at high current density using gas diffusion electrodes, *J. Appl. Electrochem.* 44 (2014) 1107-1116. doi:10.1007/s10800-014-0731-x.
- [40] G. Díaz-Sainz, M. Alvarez-Guerra, J. Solla-Gullón, L. García-Cruz, V. Montiel, A. Irabien, Gas-liquid-solid reaction system for CO₂ electroreduction to formate without using supporting electrolyte, *AIChE J.* 66 (2020) e16299. doi:10.1002/aic.16299.
- [41] C. Oloman, H. Li, Electrochemical processing of carbon dioxide., *ChemSusChem.* 1 (2008) 385–391. doi:10.1002/cssc.200800015.
- [42] A.S. Agarwal, Y. Zhai, D. Hill, N. Sridhar, The electrochemical reduction of carbon dioxide to formate/formic acid: Engineering and economic feasibility, *ChemSusChem.* 4 (2011) 1301–1310. doi:10.1002/cssc.201100220.
- [43] T. Burdyny, W.A. Smith, CO₂ reduction on gas-diffusion electrodes and why catalytic performance must be assessed at commercially-relevant conditions, *Energy Environ. Sci.* 12 (2019) 1442–1453. doi:10.1039/c8ee03134g.
- [44] M. Jouny, W. Luc, F. Jiao, General Techno-Economic Analysis of CO₂ Electrolysis Systems, *Ind. Eng. Chem. Res.* 57 (2018) 2165–2177. doi:10.1021/acs.iecr.7b03514.
- [45] R.G. Grim, Z. Huang, M.T. Guarnieri, J.R. Ferrell, L. Tao, J.A. Schaidle, Transforming the carbon economy: challenges and opportunities in the convergence of low-cost electricity and reductive CO₂ utilization, *Energy Environ. Sci.* 13 (2020) 472-494. doi:10.1039/c9ee02410g.
- [46] J.M. Spurgeon, B. Kumar, A comparative technoeconomic analysis of pathways

- for commercial electrochemical CO₂ reduction to liquid products, *Energy Environ. Sci.* 11 (2018) 1536–1551. doi:10.1039/c8ee00097b.
- [47] M. Pérez-fortes, E. Tzimas, Joint Research Center (JCR) Science for Policy Report, European Union, Luxembourg (2016). doi:10.2790/89238.
- [48] A. Dominguez-Ramos, B. Singh, X. Zhang, E.G. Hertwich, A. Irabien, Global warming footprint of the electrochemical reduction of carbon dioxide to formate, *J. Clean. Prod.* 104 (2015) 148–155. doi:10.1016/j.jclepro.2013.11.046.
- [49] F.P. García de Arquer, O.S. Bushuyev, P. De Luna, C.T. Dinh, A. Seifitokaldani, M.I. Saidaminov, C.S. Tan, L.N. Quan, A. Proppe, M.G. Kibria, S.O. Kelley, D. Sinton, E.H. Sargent, 2D Metal Oxyhalide-Derived Catalysts for Efficient CO₂ Electroreduction, *Adv. Mater.* 30 (2018) 1802858. doi:10.1002/adma.201802858.
- [50] T. Tran-Phu, R. Daiyan, Z. Fusco, Z. Ma, R. Amal, A. Tricoli, Nanostructured β -Bi₂O₃ Fractals on Carbon Fibers for Highly Selective CO₂ Electroreduction to Formate, *Adv. Funct. Mater.* 30 (2020) 1–8. doi:10.1002/adfm.201906478.
- [51] G. Liu, Z. Li, J. Shi, K. Sun, Y. Ji, Z. Wang, Y. Qiu, Y. Liu, Z. Wang, P.A. Hu, Black reduced porous SnO₂ nanosheets for CO₂ electroreduction with high formate selectivity and low overpotential, *Appl. Catal. B Environ.* 260 (2020) 118134. doi:10.1016/j.apcatb.2019.118134.
- [52] D. Li, J. Wu, T. Liu, J. Liu, Z. Yan, L. Zhen, Y. Feng, Tuning the pore structure of porous tin foam electrodes for enhanced electrochemical reduction of carbon dioxide to formate, *Chem. Eng. J.* 375 (2019) 122024. doi:10.1016/j.cej.2019.122024.
- [53] B. Ávila-Bolívar, L. García-Cruz, V. Montiel, J. Solla-Gullón, Electrochemical

Reduction of CO₂ to Formate on Easily Prepared Carbon-Supported Bi Nanoparticles, *Molecules*. 24 (2019) 2032. doi:10.3390/molecules24112032.

- [54] J. F. Moulder, W.F. Stickle, P.E. Sobol and K.D. Bomben, K. D, *Handbook of X Ray Photoelectron Spectroscopy: A Reference Book of Standard for Identification and Interpretation of Xps Data*, Physical Electronics Division, Perkin-Elmer Corporation: Eden Prairie, 1995.

Highlights

- Bi-based catalysts were used in a continuous process for CO₂ electroreduction
- The process developed offers the best trade-off among relevant figures of merit.
- FE of 90% and concentrations of 340 g·L⁻¹ of HCOO⁻ were achieved.
- At 45 mA·cm⁻², energy consumption of only 180 kWh·kmol⁻¹ was required.